eq 5, at 600 and 850 K. This yields $\alpha = 1.92 \times 10^{-11}$ cm^3 molecule^{-1} s^{-1} and $\beta = 2785$ K. Hence

$$k_1(T) = \frac{1.92 \times 10^{-11}[1 - \exp(-4157\ \mathrm{K}/T)]}{(T/\mathrm{K})^{1/2}[1 - \exp(-535\ \mathrm{K}/T)^2][1 - \exp(-739\ \mathrm{K}/T)]} \times \exp(-2785\ \mathrm{K}/T)\ \mathrm{cm}^3\ \mathrm{molecule}^{-1}\ \mathrm{s}^{-1} \quad (8)$$

This $k_1(T)$ expression is plotted in Figure 4, along with eq 5 and is seen to be in excellent agreement with the recommended $k_1(T)$ expression based on experimental data. This is consistent with the observed curvature not being due to vibrational excitation.

Also shown in Figure 4 are the results of TST and quasiclassical trajectory (QCT) calculations by Brown and Smith[11] from 300 to 600 K, and the three-dimensional QCT calculations of Persky and Broida[12] from 300 to 700 K. It is seen that there are significant differences between the resulting lines, particularly in the Arrhenius A factors. The QCT calculations of Persky and Broida are based on two different generalized LEPS surfaces, I and II. The QCT calculations of Brown and Smith are based on a simplified LEPS surface with a single adjustable parameter. It is seen from this figure that, when compared to the present $k_1(T)$ recommendation, the TST calculations of Brown and Smith overestimate the k_1 values approximately by factors of 2-3. In contrast, the QCT calculations of Persky and Broida underestimate the k_1 values approximately by factors of 1.5-4. The QCT calculations of Brown and Smith are, however, seen to be in good agreement with the present $k_1(T)$ recommendation over the range of temperature overlap. However, these authors noted that such agreements may be fortuitous.

Acknowledgment. This work was supported by the Department of Energy, Office of Basic Energy Sciences, under Grant DE-FG02-84ER13224. We thank W. F. Flaherty for constructing the newly designed HTP reactor and T. Ko for helpful suggestions.

Registry No. O, 17778-80-2; HCl, 7647-01-0.

Kinetic and Thermochemical Studies of the Recombination Reaction Na + O_2 + N_2 from 590 to 1515 K by a Modified High-Temperature Photochemistry Technique

Paul Marshall,† A. S. Narayan, and Arthur Fontijn*

High-Temperature Reaction Kinetics Laboratory, Department of Chemical Engineering, Rensselaer Polytechnic Institute, Troy, New York 12180-3590 *(Received: September 1, 1989; In Final Form: November 9, 1989)*

An adaptation of the HTP (high-temperature photochemistry) technique to make it suitable for the study of metal atoms is described. In this, the first such HTP work, sodium salts are evaporated and ground-state atomic Na is generated by pulsed excimer or flash lamp photolysis. The decay of [Na] under pseudo-first-order conditions in the presence of O_2 is monitored by time-resolved resonance absorption at 589 nm and total N_2 pressures from 40 to 320 mbar. For the reaction Na + O_2 + N_2 → NaO_2 + N_2 (1), we thus determine log k(590-1515 K) = -44.29 + 11.70 log T - 2.347(log T)^2 (cm^6 molecule^{-2} s^{-1}) with a 2σ confidence interval of 21-26%, depending on temperature, which figures include a liberal allowance for potential systematic errors. Agreement with other studies of reaction 1 in isolation, over more limited temperature ranges, is good in regions of overlapping temperatures, but simple empirical extrapolations of the various data sets deviate. Results of calculations based on a Troe formalism for energy transfer well describe the present and most of these previous $k(T)$ determinations. No evidence of equilibration of reaction 1 is observed, from which we conclude that the bond energy D_0(Na-O_2) ≥ 230 ± 5 kJ mol^{-1}, in accord with a recent flame modeling study but not with the ab initio calculations presented.

1. Introduction

In previous work, we have developed two techniques for the study of isolated elementary reactions at high temperatures (here defined as $T \gtrsim 1000$ K). Both techniques can be employed, dependent upon the compounds used, over the approximately 300-1900 K temperature range. The pseudostatic HTP (high-temperature photochemistry) technique has been used for measurements on reactions of species such as O and H, obtained by photolysis from permanent gases.[1-4] In that technique, collisions with the hot reactor walls essentially only occur for reactants that remain outside the observation zone. The HTFFR (high-temperature fast-flow reactor) technique has been used for the study of atoms and radicals of metallic elements such as Fe, Ge, Al, AlO, and AlCl, usually obtained by high-temperature vaporization methods.[5-11] These studies have provided the only kinetic information on isolated elementary reactions of metallic species available above about 1000-1100 K. We have now modified the HTP technique to allow vaporization of metal compounds, which upon photolysis produce the desired atoms, in order to (i) provide by an independent technique comparisons at the higher temperatures to HTFFR results and (ii) study metal atoms, not themselves compatible with high-temperature reaction tube walls.

For the first study, we have selected the reaction

$$\mathrm{Na} + \mathrm{O_2} + \mathrm{N_2} \rightarrow \mathrm{NaO_2} + \mathrm{N_2} \quad (1)$$

Earlier attempts to study this reaction at high temperatures in an HTFFR failed, as the Na atoms were reversibly adsorbed by the alumina reactor walls.[12] Reaction 1 is both of atmospheric and combustion interest.[13-16] In recent studies, (1) has been

† Theoretical analysis made at present address: Department of Chemistry, University of North Texas, P.O. Box 5068, Denton, TX 76203-5068.

(1) Marshall, P.; Fontijn, A. *J. Chem. Phys.* **1986**, *85*, 2637.
(2) Mahmud, K.; Marshall, P.; Fontijn, A. *J. Phys. Chem.* **1987**, *91*, 1568.
(3) Marshall, P.; Ko, T.; Fontijn, A. *J. Phys. Chem.* **1989**, *93*, 1922.
(4) Mahmud, K.; Fontijn, A. *22nd Symposium (International) on Combustion*; The Combustion Institute: Pittsburgh, 1989; p 991.
(5) Fontijn, A. *Spectrochim. Acta* **1988**, *43B*, 1075.
(6) Rogowski, D. F.; Fontijn, A. *21st Symposium (International) on Combustion*; The Combustion Institute: Pittsburgh, 1986; p 943.
(7) Rogowski, D. F.; Fontijn, A. *Chem. Phys. Lett.* **1986**, *132*, 413.
(8) Rogowski, D. F.; Marshall, P.; Fontijn, A. *J. Phys. Chem.* **1989**, *93*, 1118.
(9) Fontijn, A. *Combust. Sci. Technol.* **1986**, *50*, 151.
(10) Fontijn, A.; Felder, W. In *Reactive Intermediates in the Gas Phase*; Setser, D. W., Ed.; Academic: New York, 1979; Chapter 2.
(11) Fontijn, A.; Felder, W. *J. Chem. Phys.* **1980**, *72*, 4315.
(12) Fontijn, A. Some Measurements of the Kinetics of the Na/O_2/M Reaction. AeroChem Research Laboratories, Inc., Princeton, NJ, TP-324, final report to Sandia Co., Albuquerque, NM, 1975.

0022-3654/90/2094-2998$02.50/0

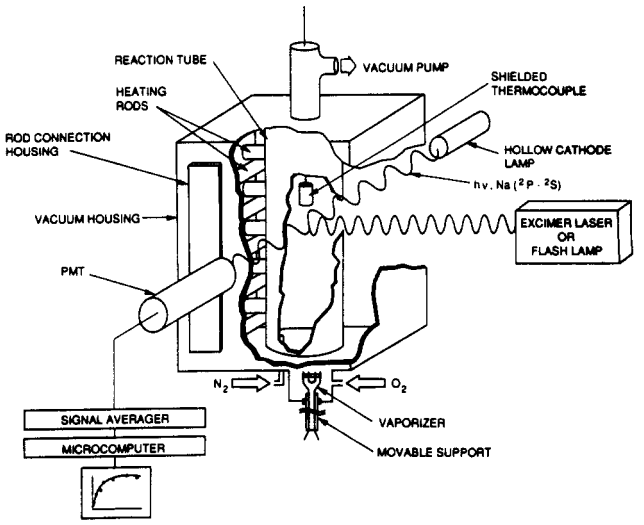

Figure 1. Schematic of the modified HTP reactor.

observed in isolated reaction environments, over respectively the 300–700,[15] 415–1016,[13,14] and 233–1118 K[16] ranges. These investigations showed reasonable agreement with each other at the same temperatures but suggested different extrapolations to higher and lower temperatures. Other recent work[17,18] has suggested that the $D_0(Na–O_2) \leq 184$ kJ mol^{-1} values previously accepted are too low. By observing the (absence of) equilibration effects in the present measurements, at higher temperatures than used in earlier isolated reaction studies, we show here substantial agreement with the highest reported value.[17]

2. Technique

2.1. Experimental Method and Conditions. The reactor is shown in Figure 1. The alumina reaction tube, 5-cm i.d., 38-cm length, is housed inside a water-cooled stainless steel vacuum housing 21 × 21 cm, 42-cm length. Heating is provided by 20 SiC 1.0-cm-diameter resistance rods, stacked alternately at right angles. The rods are introduced through the offset water-cooled rod connection housing, where the electrical contact with the cable from the variable autotransformer is made. This type of heating system differs from that used in earlier HTP designs but has been found in recent HTFFR studies[6,7,19] to give the most reliable operation in the 1500–1900 K temperature regime. Zircar insulation (not shown) is placed between the central hottest parts of the rods and the housing; the cooler ends pass through the insulation. The reaction tube has four circular 2-cm-diameter openings aligned with the 1.9-cm-diameter windows in the vacuum housing. The temperature of the reaction zone, axially defined by the window section, is measured before and after each experiment with a retractable Pt/Pt–13% Rh thermocouple doubly shielded to minimize radiation errors.[10,20] The basic difference with previous HTP work is that the cooled inlet for thermally unstable reactants is replaced by an alumina or boron nitride crucible, for evaporation of the photolyte, mounted on a movable support. In some experiments the crucibles are heated directly by the reactor walls, in which case their rim is situated about 10 cm from the center of the reaction zone. In others they are retracted in the tubular section extending below the main housing, in which case they can be heated by a tungsten electrical resistance coil; this distance is about 29 cm. In this manner the photolyte flow can be controlled independently of the reactor temperature.

A Questek Model 2610 excimer laser, operated at 193 nm, or a flash lamp[2] is used for the photolysis. Both are operated at about 1 Hz. Laser pulse energy varied from 25 to 250 mJ. The 25-mJ pulses are attenuated by factors up to about 100, with neutral density filters made from overlapping metal gauzes. A Suprasil quartz lens is used as the entrance window of the reactor to spread the laser beam, which is initially 1 cm high. This divergence causes the Na to be created in a 2.5-cm length at the center of the reaction tube, which serves three purposes: (i) the entire cross section of this probe beam is attenuated by resonance absorption, (ii) Na is lost more slowly by diffusion from the larger volume, and (iii) sweeping of Na out of the reaction zone by the gas flow is minimized. The flash lamp operates on about 270 mbar of N_2 at 10–70-J input energy/flash; photolysis conditions are further varied by using either a Suprasil or Vycor entrance window, which restricts the photolytic radiation to $\lambda \gtrsim 160$ and 220 nm, respectively.[21] [Na] is measured in absorption with a Westinghouse hollow cathode lamp. The 589.0-nm Na D-line is viewed by the PMT (photomultiplier tube) through a 589.0 ± 0.1-nm (fwhm) interference filter. In a few experiments, the filter was replaced by a monochromator to allow observation of nearby Ne lines to check for scattered light interference from particulate matter, i.e., to ascertain that no significant amounts of particulates were present. At high temperatures, the radiation from the hot reactor walls became of comparable intensity to that of the hollow-cathode lamp. To minimize this interference, in some experiments, 0.1-cm-i.d. alumina collimating tubes were placed in front of the PMT. In later work, at the highest temperatures, the following combination of changes was found to give the best results. A lens in front of hollow cathode lamp focused the light in the front of the reaction zone. The diverging beam after this point filled the PMT viewing area. Additional filters (Corning CS 4-72/3-66/1-56) transmitting from 550–600 nm, were placed in front of the PMT.

The output current from the photomultiplier tube is fed through a 10-MΩ resistor, and the resulting voltage is measured by a Nicolet Model LAS 12/70 signal averager, triggered from the excimer laser/flash lamp. The maximum sampling rate is 0.5 MHz, and 512 time channels are employed. The PMT outputs following 50–100 consecutive pulses are averaged and stored digitally. The data are then transferred to an IBM PC for analysis. [Na] is determined by the Lambert–Beer law

$$I = I_0 \exp(-\epsilon[\mathrm{Na}]l) \qquad (2)$$

where ϵ is the absorption coefficient, l the length of the absorption path, and I_0 the intensity in the absence of Na. Husain and Plane[22] showed eq 2 to be valid for $I > 0.6I_0$, using the Na D-line *doublet* at about 390 K; the higher temperatures and the single resolved line employed here further ensure its validity for degrees of absorption up to 40%. In Table I, our experimental conditions are shown, from which it may be seen that absorption lower than 40% is used in the present work. Using $\epsilon = 1.25 \times 10^{-12}$ cm^2 molecule^{-1},[22,23] we find that the initial Na concentrations, $[\mathrm{Na}]_{in}$, used in this work varied from 6.1×10^9 molecules cm^{-3} at 1% absorption to 1.9×10^{11} molecules cm^{-3} at 26% absorption.

Bath gas N_2 (99.998%; Airco) obtained from the liquid and O_2 (99.6%; Linde) were introduced as shown in Figure 1. In a few experiments, O_2 was introduced downstream from the vaporizer crucible through a small tube. The photolytes used were NaCl (ACS reagent grade) and NaI (certified grade, Fisher).

2.2. Data Handling. The decrease in [Na], after the essentially instantaneous generation of Na atoms by each photolysis pulse,

(13) Husain, D.; Marshall, P.; Plane, J. M. C. *J. Photochem.* **1986**, *32*, 1.
(14) Husain, D.; Marshall, P.; Plane, J. M. C. *J. Chem. Soc., Faraday Trans. 2* **1985**, *81*, 301.
(15) Silver, J. A.; Zahniser, M. S.; Stanton, A. C.; Kolb, C. E. *20th Symposium (International) on Combustion*; The Combustion Institute: Pittsburgh, 1984; p 605.
(16) Plane, J. M. C.; Rajasekhar, B. *J. Phys. Chem.* **1989**, *93*, 3135.
(17) Steinberg, M.; Schofield, K. The High-Temperature Chemistry and Thermodynamics of Alkali Metals (Lithium, Sodium and Potassium) in Oxygen Rich Flames, Preprint; Western Section, The Combustion Institute: Pittsburgh, November, 1987.
(18) Plane, J. M. C.; Rajasekhar, B.; Bartolotti, L. *J. Phys. Chem.* **1989**, *93*, 3141.
(19) Slavejkov, A. G.; Stanton, C. T.; Fontijn, A. *J. Phys. Chem.*, in press.
(20) Fontijn, A.; Felder, W. *J. Phys. Chem.* **1979**, *83*, 24.
(21) Okabe, H. *Photochemistry of Small Molecules*; Wiley-Interscience: New York, 1978; p 180.
(22) Husain, D.; Plane, J. M. C. *J. Chem. Soc., Faraday Trans. 2* **1982**, *78*, 163.
(23) Maissel, L. I.; Glang, R. *Handbook of Thin Film Technology*; McGraw-Hill: New York, 1970; p 1-17.

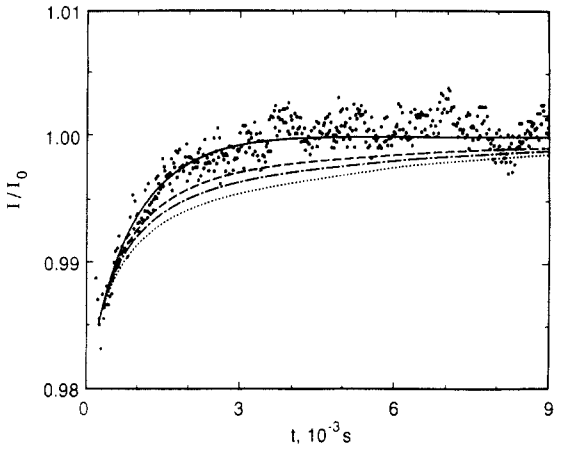

Figure 2. Plot of transmitted light intensity vs time at 1513 K, $[O_2] = 9.7 \times 10^{15}$ cm^{-3} $[N_2] = 6.2 \times 10^{17}$ cm^{-3}, to yield $k_{ps1} = 1089$ s^{-1}: (●) measured points; (—) experimental fit, eq 4, (···) equilibrium fit obtained assuming $D_0(Na-O_2) = 225$ kJ mol^{-1}, eqs 2 and 8; (-·-) equilibrium fit obtained assuming $D_0(Na-O_2) = 230$ kJ mol^{-1}, eqs 2 and 8; (- -) equilibrium fit obtained assuming $D_0(Na-O_2) = 235$ kJ mol^{-1}, eqs 2 and 8.

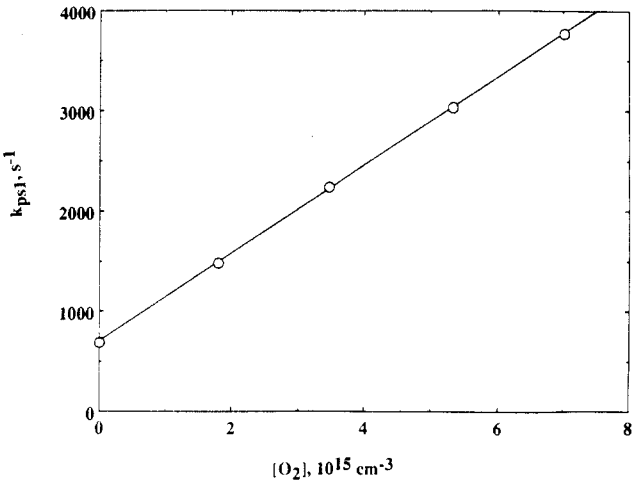

Figure 3. Plot of pseudo-first-order rate coefficient vs $[O_2]$ at fixed $[N_2]$, to yield the pseudobimolecular rate constant, k_{ps2}.

is due to reaction 1 and losses by diffusion and flow. Thus, under the pseudo-first-order conditions used $[Na] \ll [O_2]$, similar to earlier HTP work,[1-4]

$$-\frac{d}{dt}[Na] = k[Na][O_2][N_2] + k_D[Na] = k_{ps1}[Na] \quad (3)$$

where k_D represents loss other than by reaction (mainly by diffusion) and k_{ps1} is the pseudo-first-order rate coefficient. Combining eqs 2 and 3 yields an expression for I as a function of time,

$$I = I_0 \exp[-c \exp(-k_{ps1}t)] \quad (4)$$

where c is a constant. I_0 is obtained from measurements of I at large observation times, i.e., $t > 5/k_{ps1}$. A nonlinear least-squares fitting routine[24] is then used to evaluate the values of k_{ps1} and c from measurements of I/I_0 as a function of t, Figure 2. Thus, absolute [Na] is not used in the k_{ps1}, and hence k, measurements.

To measure k at a particular temperature T, k_{ps1} values are obtained for about five different $[O_2]$, running from zero to $[O_2]_{max}$, while keeping the pressure, i.e., $[N_2]$, constant. $[N_2]$ is typically 100 times greater than $[O_2]_{max}$. To find $k_{ps2} \pm \sigma_{k_{ps2}}$, the pseudo-second-order rate coefficient and its standard deviation, k_{ps1} is plotted against $[O_2]$, e.g., Figure 3, using the weighted linear fitting algorithm of Irvin and Quickenden.[25] This involves taking into account the standard deviations of k_{ps1} and $[O_2]$. $\sigma_{k_{ps1}}$ is taken to be 10% of k_{ps1} on the basis of the observed scatter and reproducibility of the decay profiles. $\sigma_{[O_2]}$ arises mainly from the uncertainty in the flow meter readings, which are about 1.5% in full scale. The third-order-rate coefficient k is then found by dividing k_{ps2} by $[N_2]$, which value is entered as one line in Table I. To check that $k_{ps2} \propto [N_2]$, i.e., that the termolecular reaction 1 was observed, plots of k_{ps2} vs $[N_2]$ were made at several temperatures. An example is shown as Figure 4.

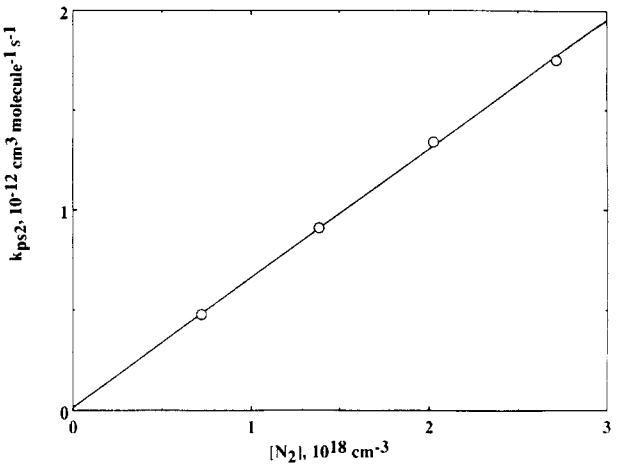

Figure 4. Plot of pseudobimolecular rate constant vs $[N_2]$, to verify third-order behavior.

To find $k(T)$, σ_k is taken to be $\sigma_{k_{ps2}}/[N_2]$, as variations in $[N_2]$ are negligible (<1%). We again estimate, as in previous work,[1,4] $\sigma_T/T = 2\%$. Because this temperature uncertainty affects both $[N_2]$ and $[O_2]$ in the same direction, it contributes an extra 4% to the uncertainty in k. To accommodate curvature in the plot of log $k(T)$ vs log T and to compare to theory (see section 3.2), the data are fitted to the expression

$$\log k(T) = A + B \log T + C(\log T)2 \quad (5)$$

with the CURFIT algorithm described by Bevington,[26] to yield A,B,C and the associated variances and covariances.[27] To use this algorithm here, σ_k and σ_T are transformed to $\sigma_{\log k}$ and $\sigma_{\log T}$.[28] Each log k and log T pair is then weighted according to the statistical factor $[\sigma_{\log k}^2 + x^2\sigma_{\log T}^2]^{-1}$, where x is d log k/d log T.

3. Results and Discussion: Kinetics

3.1. Experimental Results. The 86 measurements of k made are summarized in Table I. The results may be seen to be independent of the average gas velocity $\bar{v}$, varied from 10 to 47 cm s^{-1}, and whether the vaporizer was in the heated zone or retracted. Together these factors show the independence of residence time and demonstrate that adequate mixing and thermal equilibration are achieved. We further find the results shown to be independent of (i) $[Na]_{in}$, (ii) the photolysis source used and the variation in its energy output, as well as whether the actinic radiation passed through Vycor or Suprasil (iii) the photolyte used (NaI or NaCl), (iv) the method of introduction of O_2 (upstream or downstream of the vaporizer), and (v) the type of wavelength isolation used (interference filter or monochromator). However, we find at temperatures above ≈1000 K with 193-nm laser photolysis that the results become dependent on the photolyte used and tend toward a second-order rather than third-order rate coefficient, apparently due to secondary photochemical effects. No such problems were encountered with the flash lamp, which was

(24) Marshall, P. Ph.D. Thesis, University of Cambridge, 1985.
(25) Irvin, J. A.; Quickenden, T. I. *J. Chem. Educ.* **1983**, *60*, 711.
(26) Bevington, P. R. *Data Reduction and Error Analysis for the Physical Sciences*; McGraw-Hill: New York, 1969; Chapter 11.
(27) Wentworth, W. E. *J. Chem. Educ.* **1965**, *42*, 96.
(28) Bevington, P. R. *Data Reduction and Error Analysis in the Physical Sciences*; McGraw-Hill: New York, 1969; Chapter 4.

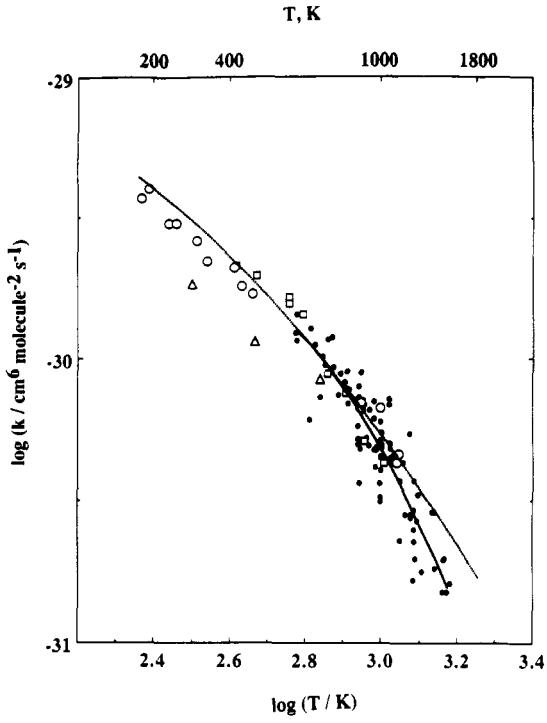

Figure 5. Comparison of present rate coefficients measurements with theory and previous results: (●) present study; (△) Silver et al.; (□) Husain et al.; (○) Plane et al.; (—) best fit to present study, eq 6; (···) theoretical estimate, eq 7.

therefore exclusively used at the higher temperatures.

Introducing the k measurements in eq 5 yields

$$\log k(T) = -44.29 + 11.70 \log T - 2.347(\log T)^2 \quad \text{cm}^6 \text{ molecule}^{-2} \text{ s}^{-1} \tag{6}$$

The variances for the parameters A, B, and C are

$$\sigma_A^2 = 44.21, \quad \sigma_B^2 = 20.14, \quad \sigma_C^2 = 0.573$$

with associated covariances

$$\sigma_{AB} = -29.83, \quad \sigma_{AC} = 5.03, \quad \sigma_{BC} = -3.39$$

The variances and covariances are combined by the method of Wentworth.[27] This, along with the transformation $\sigma_k = 2.303k\sigma_{\log k}$,[28] yields a confidence interval for $k(T)$ varying from ±6% at 900 K increasing to ±17% at the extremes of the present temperature range at the 2σ level. Allowing conservatively for systematic errors of ±20% increases the confidence limits to ±21% and ±26%, respectively. In Figure 5, these data points and the fit expression are shown together with the results of previous studies of reaction 1 in isolation, i.e., not in flames or other multireaction media. Agreement of the present k results, in the regions of overlapping temperature, with the flash photolysis/resonance absorption experiments of Husain et al.[13,14] and the flash photolysis/laser-induced fluorescence work of Plane and Rajasekhar[16] is good and is within the uncertainty limits. There is also good accord with the 700 K flow-tube measurements of Silver et al.,[15] although at lower temperatures the flow-tube results lie about 40% below the flash photolysis results. Figure 5 also shows that simple empirical extrapolations of the different data sets do *not* agree.

3.2. Theoretical Estimates of k. We have carried out kinetic calculations for reaction 1 using the Troe formalism for an energy-transfer mechanism, as employed in earlier work.[13,14,16] This mechanism is based on the initial formation of excited NaO_2*, which is then stabilized by collision with the bath gas. Input parameters that must be chosen are D_0, the temperature dependence of the mean energy transferred $\langle \Delta E \rangle$ per stabilizing collision, and the two Lennard-Jones parameters σ_{LJ} and ϵ_{LJ}, which characterize these collisions. The procedure is to calculate the low-pressure bimolecular decomposition rate coefficient of NaO_2 and to derive the termolecular association rate coefficient k via the equilibrium constant. Details of the calculations, and other parameters, have been given earlier.[13,14] Here, we employ D_0 = 230 kJ mol^{-1} (see section 4.1), fit the formalism to the measured k at T = 700 K, and, for simplicity, assume $\langle \Delta E \rangle$ to be temperature independent. We find that selection of σ_{LJ} = 0.35 nm and ϵ_{LJ}/k_B = 300 K gives the best agreement with our results, at least up to 1300 K, and most previous rate coefficient data:[13-16] this accord is demonstrated on Figure 5. The calculated k values can be summarized to within 4% over the 200–1800 K range, by the expression

$$\log k(T) = -30.33 + 1.855 \log T - 0.6111(\log T)^2 \quad \text{cm}^6 \text{ molecule}^{-2} \text{ s}^{-1} \tag{7}$$

Similar agreement with experiment has been found previously, with use of slightly different Lennard-Jones potentials, for D_0 = 170 kJ mol^{-1} [13,14] and D_0 = 202 kJ mol^{-1}.[16] Thus, the temperature dependence of k does not critically depend on the value of D_0, even over the wide temperature range from 230 to 1515 K, for which data are now available. Physically, this is because the effects of D_0 on the unimolecular decay of NaO_2 and the equilibrium constant of reaction 1 largely cancel. In view of the difficulty of determining D_0 (see section 4), the independence of the calculated k from D_0 is perhaps fortunate and means that ab initio estimates of the rate coefficients of similar reactions may be reliable enough for use in combustion modeling.

4. Results and Discussion: Thermochemical Results

4.1. Experimental Results. The kinetic analysis described in section 2 is based upon the forward reaction 1 only, with a negligible back-reaction. All the observed I vs t profiles fit the form of eq 4, so we find no evidence of reaction 1 coming to equilibrium with a nonzero Na concentration. Here, we quantify this observation as a lower limit on K_c, the equilibrium constant for reaction 1, and derive a lower limit for D_0. Because $[Na]_{in} \ll [O_2]$, we can write $K_c = f/\{(1-f)[O_2]\}$ where f is the fraction of Na removed by reaction with O_2, in the absence of any loss of Na by diffusion. The absence of equilibration corresponds to f = 1. Choice of the *lowest* f value still consistent with the observation that $f \approx 1$ is somewhat arbitrary. A more detailed analysis that includes diffusion, presented below, supports values of f of about 0.67–0.75 and higher. Table II shows the K_c values corresponding to f = 0.67, obtained from individual I vs t profiles, under conditions where equilibrium would have been most obvious, i.e., at the lowest nonzero $[O_2]$ at the highest temperatures. Limiting D_0 values are calculated from each K_c statistical mechanically, with bond lengths and vibrational frequencies used earlier:[14] r(O–O) = 133 pm, r(Na–O) = 207 pm, ν_1 = 332.8 cm^{-1}, ν_2 = 390.7 cm^{-1}, and ν_3 = 1080 cm^{-1}. Naturally, the higher the temperature at which equilibration is *not* observed, the higher the limit on D_0, as seen in Table II. The values in Table II suggest D_0 is at least 225–230 kJ mol^{-1}.

As a more detailed check on whether the I vs t profiles support this value, we calculate the profile expected at 1513 K if D_0 = 230 kJ mol^{-1} (corresponding to f = 0.67), which is shown in Figure 2. Calculation of the model profile allows for diffusion of both Na and NaO_2 out of the reaction zone, which will cause the limiting value of [Na] to be zero, even in the absence of equilibration. We employ a kinetic analysis based upon equal diffusion rates for reactants and products, which yields[29]

$$\epsilon[Na]I = a_1 \exp[-(k_1[O_2][N_2] + k_{-1}[N_2] + k_D)]t + a_2 \exp[-(k_D)t] \tag{8}$$

where a_1, a_2, and k_{-1} are found from

$$K_c = a_1/\{a_2[O_2]\} = k_1/k_{-1} \tag{9}$$

$$a_1 + a_2 = \epsilon[Na]_{in}I \tag{10}$$

(29) Balla, R. J.; Weiner, B. R.; Nelson, H. H. *J. Am. Chem. Soc.* **1987**, *109*, 4804.

TABLE I: Summary of Rate Coefficient Measurements for Na + O_2 + N_2

T, K	P, mbar	$[M] \approx [N_2]$, 10^{18} cm^{-3}	$[Na]_{in}$, % abs	$[O_2]_{max}$, 10^{15} cm^{-3}	$\bar{v}$, cm s^{-1}	$k \pm \sigma_k$, 10^{-31} cm^6 molecule^{-2} s^{-1}	conditions[a]
593	95	1.2	6	7.0	12	12.4 ± 0.5	a, e, f
597	59	0.72	13	9.4	17	11.7 ± 1.0	
598	45	0.55	11	8.2	19	14.4 ± 1.0	
649	171	1.9	4	6.9	13	6.1 ± 0.4	a, e, f
650	40	0.45	14	10.5	17	12.8 ± 1.1	
669	67	0.73	18	9.9	17	11.2 ± 0.9	
693	71	0.73	7	5.3	16	7.3 ± 1.4	a, b, e
700	109	1.1	11	7.7	15	10.2 ± 0.6	
708	107	1.1	14	17.1	10	9.5 ± 0.8	
723	37	0.37	14	6.8	24	11.8 ± 0.6	
741	55	0.54	11	9.0	17	11.9 ± 1.1	a, e, f
747	77	0.75	13	11.5	17	9.4 ± 0.6	
771	191	1.8	11	6.4	16	7.5 ± 0.5	
783	92	0.86	7	7.6	16	8.9 ± 0.8	a, b, e
802	129	1.2	9	14.8	20	8.3 ± 0.5	
815	79	0.71	12	10.1	17	9.0 ± 0.5	
816	148	1.3	12	15.4	16	7.9 ± 0.5	
820	125	1.1	13	8.4	21	7.5 ± 0.5	c, e
822	191	1.7	15	8.9	20	7.0 ± 0.6	c, e
823	71	0.62	26	9.1	20	7.8 ± 0.7	c, e
852	93	0.80	17	17.5	20	7.2 ± 0.8	
871	131	1.1	5	6.7	20	5.2 ± 0.6	c, e
871	131	1.1	25	6.7	20	5.8 ± 0.3	c, e
872	209	1.7	8	5.5	16	5.0 ± 0.5	c, e
873	121	1.0	6	6.2	24	3.6 ± 0.4	a, e, f
874	80	0.66	15	7.0	19	6.7 ± 0.3	c
874	80	0.66	14	7.0	19	7.3 ± 0.4	c, e
875	133	1.1	13	6.9	20	8.0 ± 0.7	c, e
879	164	1.4	8	11.4	19	4.8 ± 0.7	a, d
887	44	0.36	13	15.1	17	9.0 ± 0.8	a, d, f
888	53	0.44	9	6.5	27	6.5 ± 0.5	
893	93	0.76	23	8.3	20	6.8 ± 0.4	c, e, f
900	128	1.0	10	17.0	21	6.6 ± 0.5	
901	129	1.0	15	10.2	18	7.2 ± 0.5	c, e, f
904	79	0.63	7	18.7	19	6.9 ± 0.6	
918	132	1.0	17	7.4	20	5.3 ± 0.3	
926	63	0.49	11	12.4	14	5.0 ± 0.4	
934	68	0.53	15	24.0	15	6.6 ± 0.5	
960	115	0.86	17	9.6	19	7.1 ± 0.5	c, e, f
961	163	1.2	13	8.4	20	6.2 ± 0.3	c, e, f
961	79	0.60	13	9.8	17	4.8 ± 0.3	
967	41	0.30	16	8.3	22	4.1 ± 0.3	
971	68	0.51	14	7.0	27	4.8 ± 0.4	
973	223	1.7	15	8.0	21	4.9 ± 0.3	c, e, f
994	321	2.3	21	9.2	21	3.6 ± 0.3	c, e, f
995	43	0.31	9	20.4	23	4.5 ± 0.4	
996	143	1.0	11	8.0	21	5.2 ± 0.4	c, e, f
997	261	1.9	17	8.6	20	4.1 ± 0.3	c, e, f
997	127	0.92	8	19.5	20	3.1 ± 0.3	
998	192	1.4	16	16.4	22	6.0 ± 0.4	c, e
998	200	1.5	11	7.4	22	4.5 ± 0.3	c, e
1001	51	0.37	14	7.6	27	3.3 ± 0.3	
1002	47	0.34	10	7.4	21	5.5 ± 1.0	c, e
1002	128	0.93	9	6.8	21	5.0 ± 0.4	c, e
1002	128	0.93	11	6.8	21	4.9 ± 0.4	c
1046	83	0.57	15	14.8	22	4.3 ± 0.4	a, d, f
1050	71	0.49	17	8.2	30	7.2 ± 0.6	a, b
1051	117	0.81	18	14.6	18	6.9 ± 0.9	a, b
1055	47	0.32	16	16.3	22	4.8 ± 0.5	
1055	219	1.5	14	12.8	22	4.5 ± 0.3	a, d
1056	77	0.53	14	10.4	25	5.0 ± 0.6	a, d
1078	148	0.99	15	4.1	39	4.6 ± 1.0	a, h
1119	49	0.32	21	13.7	22	3.7 ± 0.5	a, d, f
1121	84	0.54	12	16.5	18	2.3 ± 0.2	a, d, f
1145	69	0.44	9	8.4	21	4.3 ± 0.2	a, d, g
1159	196	1.2	12	12.5	22	2.8 ± 0.2	a, d, g
1188	68	0.42	8	14.4	35	5.4 ± 0.4	a, b, g
1201	161	0.98	12	8.4	30	2.7 ± 0.1	a, h
1202	117	0.71	13	15.9	22	2.8 ± 0.4	a, h
1213	132	0.78	9	6.6	19	1.7 ± 0.1	a, h
1219	141	0.84	16	15.1	19	2.9 ± 0.3	a, d, g
1219	215	1.3	16	14.0	21	2.3 ± 0.1	a, d, g
1222	140	0.84	11	3.4	43	2.5 ± 0.3	a, h
1225	69	0.41	14	16.3	20	3.7 ± 0.3	a, d, g
1228	140	0.82	9	15.9	20	2.0 ± 0.3	a, d, g
1250	92	0.53	3	12.7	25	2.7 ± 0.3	a, h

TABLE I (Continued)

T, K	P, mbar	$[M] \approx [N_2]$, 10^{18} cm^{-3}	$[Na]_{in}$, % abs	$[O_2]_{max}$, 10^{15} cm^{-3}	$\bar{v}$, cm s^{-1}	$k \pm \sigma_k$, 10^{-31} cm^6 molecule^{-2} s^{-1}	conditions[a]
1257	189	1.1	14	8.9	30	3.3 ± 0.4	a, h
1280	109	0.62	9	18.0	21	1.8 ± 0.1	a, h
1368	83	0.43	1	9.4	47	2.9 ± 0.4	a, c, f, h
1382	108	0.56	1	13.9	19	2.9 ± 0.2	a, c, f, h
1388	152	0.79	5	15.1	29	1.8 ± 0.1	a, c, f, h
1452	201	1.0	20	20.8	25	1.5 ± 0.1	a, f, g
1460	115	0.57	14	22.4	25	2.0 ± 0.2	a, f, g
1466	156	0.77	12	20.8	26	2.0 ± 0.2	a, f, g
1491	128	0.62	1	16.6	46	1.5 ± 0.1	a, c, f, h
1513	128	0.62	1	15.9	36	1.6 ± 0.3	a, c, f, h

[a] Conditions under which the experiment is performed (If not mentioned otherwise, the data are obtained with the excimer laser, the quartz lens, crucible retracted, the interference filter, oxygen introduced upstream of the photolyte source, and NaI as photolyte.): (a) flash lamp used for photolysis; (b) Vycor window separated flash lamp from reactor; (c) crucible inside the heated zone; (d) isolation of the 589-nm line by the monochromator; (e) oxygen introduced downstream of the crucible; (f) NaCl as the photolyte; (g) collimator tubes placed in front of the PMT; (h) lens in front of hollow cathode lamp and additional 550–600-nm-filter combination in front of the photomultiplier tube.

TABLE II: Thermochemistry of NaO_2 Obtained from Direct Observation of [Na][a]

T, K	$[O_2]$, 10^{15} cm^{-3}	lower limit to K_c, 10^{-16} cm^3	lower limit to D_0, kJ mol^{-1}
1452	7.3	2.7	225
1460	6.5	3.1	227
1466	5.5	3.6	230
1513	9.4	2.1	230

[a] At least 0.67 of the initial Na is assumed to react with O_2.

$\epsilon[Na]l$ is then substituted in eq 2, yielding a plot of I/I_0 vs t. As seen in Figure 2, the observed data points lie significantly above the profile calculated for D_0 = 230 kJ mol^{-1}.[30] Repetition of this procedure for D_0 = 235 and 225 kJ mol^{-1}, Figure 2, (corresponding to f = 0.57 and 0.75) yields a lesser and larger deviation, respectively. We conclude that a valid lower limit to D_0 is 230 ± 5 kJ mol^{-1}.

The above analysis relies on reaction 1 dominating chemical removal of Na. Two other potential chemical routes must be eliminated. The first possibility is that of a secondary reaction removing Na or NaO_2 (so that equilibrium is never reached), perhaps Na + NaO_2 or NaO_2 + NaO_2. Because $[Na]_{in} < 2 \times 10^{11}$ cm^{-3}, even if the reaction has a rate coefficient of 10^{-10} cm^3 molecule^{-1} s^{-1}, the maximum possible contribution to the observed k_{ps1} is less than 20 s^{-1}, which is too small to account for the loss of Na (compare Figure 2). The second possible removal route is for [Na] to be shifted by the reaction $NaO_2 + O_2 \rightleftharpoons NaO_4$. However, the O_2–NaO_2 bond energy is thought to be low, about 40 ± 20 kJ mol^{-1},[31] so this molecule is an unlikely sink for NaO_2 at temperatures above 1400 K.

4.2. Comparison of Results with Earlier Measurements. Our limiting value for D_0 is compared to previous experimental estimates in Table III. The earlier results were obtained by four techniques: (i) direct observation of [Na] vs t in isolated reaction systems, as here; (ii) modeling of [Na] profiles in flames; (iii) observation of chemiluminescence from crossed beams of Na_2 and O_2; and (iv) mass spectrometer measurements on effusing vapor from a Knudsen cell. Table III shows that the results for lower limits on D_0 derived from direct observation depend on the temperature range employed: our limit of 230 ± 5 kJ mol^{-1} from work at 1515 K is higher than previous limits from lower temperature experiments: the work of Husain and Plane[22] at 840 K, as interpreted by Jensen,[32] yields $D_0 \geq$ 145 kJ mol^{-1}, and the work of Plane and Rajasekhar[18] at 1120 K yields $D_0 \geq$ 202 kJ mol^{-1}.

The modeling of sodium-seeded flames is vulnerable to uncertainties in the assumed Na reaction mechanism. For example, the flame experiments of McEwan and Phillips,[33] as later reanalyzed,[34] yielded D_0 = 234 ± 13 kJ mol^{-1}, but this value is in only fortuitous agreement with the present work because the estimate of k then current[35] is 3 orders of magnitude too small. The flame modeling by Jensen,[32] in which the dominant Na-removal reaction was assumed to be with OH, yielded $D_0 \leq$ 195 kJ mol^{-1}. Subsequently, Hynes et al.[36] gave larger emphasis to reaction 1 and estimated D_0 = 163 ± 21 kJ mol^{-1}. The most recent modeling study by Steinberg and Schofield,[17] based on the best current input data, yields D_0 = 243 ± 21 kJ mol^{-1}, which is in accord with the present estimate.

TABLE III: Previous Experimental Estimates of $D_0(Na–O_2)$

D_0, kJ mol^{-1}	method	comments
≥145	direct observation of [Na]	Husain and Plane[22] data analyzed by Jensen[32]
≥202	direct observation of [Na]	Plane et al.[18]
234 ± 13	flame model	McEwan and Phillips[33] data reanalyzed by Dougherty et al.[34]
≤195	flame model	Jensen[32]
163 ± 21	flame model	Hynes et al.[36]
243 ± 21	flame model	Steinberg and Schofield[17]
≤184	chemiluminescence	Figger et al.[37]
<115	Knudsen cell	Lamoreaux and Hildenbrand[38]

The discrepancy with $D_0 \leq$ 184 kJ mol^{-1} obtained by Figger et al.[37] from the wavelength threshold of chemiluminescence from the reaction $Na_2 + O_2$ presumably indicates that their proposed mechanism must be reevaluated.

The Knudsen cell/mass spectrometer studies by Lamoreaux and Hildenbrand[38] show no detected NaO_2(g) above heated Na_2O(s). Their limiting thermochemical values, calculated on the basis of estimated detector sensitivity, imply $D_0 <$ 115 kJ mol^{-1}, in contradiction to both flame and direct results. It is therefore plausible that either NaO_2 is not formed under Knudsen cell conditions for kinetic reasons or that the NaO_2 molecule cannot be detected by mass spectrometry, perhaps because it has an unstable positive ion.

4.3. Theoretical Estimates of D_0. Alexander suggested $D_0 \approx$ 150 kJ mol^{-1} based on semiempirical arguments.[39] Figger et al. found that a Rittner model lead to D_0 = 196 kJ mol^{-1}.[37] Ab initio calculations on the NaO_2 molecule have also been made; the general approach is to select a basis set of atomic orbitals and then take linear combinations to form the molecular orbitals. These combinations are optimized until self-consistent, i.e., to the Hartree–Fock level. After the molecular geometry that minimizes

(30) If, as is likely, NaO_2 in fact diffuses more slowly than Na, then the calculated profile would deviate more strongly from the profile calculated for an effectively infinite K_c.

(31) Ager, J. W., III; Howard, C. J. *Geophys. Res. Lett.* **1986**, *13*, 1395.
(32) Jensen, D. E. *J. Chem. Soc., Faraday Trans. 1* **1982**, *78*, 2835.
(33) McEwan, M. J.; Phillips, L. F. *Trans. Faraday Soc.* **1966**, *62*, 1717.
(34) Dougherty, G. J.; McEwan, M. J.; Phillips, L. F. *Combust. Flame* **1973**, *21*, 253.
(35) Carabetta, W. R.; Kaskan, W. E. *J. Phys. Chem.* **1968**, *72*, 2483.
(36) Hynes, A. J.; Steinberg, M.; Schofield, K. *J. Chem. Phys.* **1984**, *80*, 2585.
(37) Figger, H.; Schrepp, W.; Zhu, X. *J. Chem. Phys.* **1983**, *79*, 1320.
(38) Lamoreaux, R. H.; Hildenbrand, D. L. *J. Phys. Chem. Ref. Data* **1984**, *13*, 151.
(39) Alexander, M. H. *J. Chem. Phys.* **1978**, *69*, 3502.

TABLE IV: Summary of Ab Initio MP2/6-31+ G* Calculations

bond	calculated length, pm	experimental length, pm
O–O in O_2^-	138	138,[44] 134[45]
O–O in NaO_2	139	133 ± 6[47]
Na–O in NaO_2	216	207,[47] 212[48]
species	energy, hartrees	
Na^+	−161.659 29	
O_2^-	−149.966 33	
NaO_2	−311.857 03	

$D_e(NaO_2 \rightarrow Na^+ + O_2^-)$ = 607 kJ mol^{-1}; $D_0(NaO_2 \rightarrow Na + O_2)$ = 151 kJ mol^{-1} [a]

[a] Derived from D_e using experimental data; see text.

the total energy is found, energy calculations can be performed at this geometry. Electron correlation can be estimated, for instance, at various levels of perturbation theory.

Plane et al. carried out ab initio calculations using two standard basis sets, 6-31G and 6-311G, on the dissociation to ionic products, then corrected to neutral products by means of the experimental ionization energy of Na, the electron affinity of O_2 and the zero-point energy of NaO_2.[18] Because of the ion–pair nature of NaO_2, this procedure should minimize errors in the difference between the electron correlation energies of NaO_2 and dissociation products. They optimized geometry at the Hartree–Fock level and calculated energies that incorporated correlation for valence electrons calculated from Møller–Plesset fourth-order (MP4) perturbation theory,[18] yielding D_0 = 199 and 185 kJ mol^{-1}, respectively.

Because calculations on anions are typically improved by including polarization (*) and diffuse (+) functions in the basis set,[40] we have made an ab initio analysis of D_0 with the augmented basis set of 6-31+G*, using the Gaussian 88 program.[41] This basis set represents core orbitals on each atom by six gaussian functions and splits the valence orbitals into outer and inner regions, represented by one and three gaussian functions, respectively.[42] To these functions are added d orbital polarization functions and diffuse s orbital functions.[40] Geometries are optimized with correlation calculated for all electrons at the MP2 level, followed by energy calculations at the same level. The results, given in Table IV, yield D_0 = 151 kJ mol^{-1}, which is about 80 kJ mol^{-1} below our experimental limit. Thus, all of the calculations to date yield D_0 in the range 150–200 kJ mol^{-1}, by contrast to experiment. Further work is required to resolve this conflict.

One test of the quality of the calculations is correct prediction of geometry. The calculations of O_2^- are in accord with the previous ab initio results, summarized by Besler et al.,[43] and with the larger of the two conflicting experimental determinations[44,45] of the bond length r(O–O) given in Table IV. Allen et al. recently demonstrated that r(O–O) is strongly dependent on the level of treatment of configuration interaction and derived values from 130 to 138 pm.[46] For NaO_2, there are no direct measurements of the geometry for comparison with our calculated parameters. Estimates of r(Na–O) come from an empirical correlation between force constants and bond length[47] and by fitting ESR parameters.[48] Both methods are based on data from matrix-isolation studies; the calculations presented here support the larger experimental r(Na–O).[49] The only estimate of r(O–O) in NaO_2 is the assumption that it is equal to the separation in the crystalline solid.[47] Given these uncertainties, the theoretically estimated bond lengths appear reasonable.

5. Conclusions

We have adapted the HTP technique to the study of transient metallic species. Direct rate coefficient data for reaction 1 have been obtained from 590 to 1515 K, the widest temperature range and highest temperatures to date. There is agreement between the present k values and both the previous lower temperature measurements and theoretical calculations. Absence of any observed equilibration between Na and O_2 sets a lower limit of 230 ± 5 kJ mol^{-1} for D_0(Na–O_2), in accord with the most recent model of a sodium-seeded flame. Ab initio calculations on the NaO_2 molecule agree with the limited available structural information, but there is unresolved disagreement with the experimental D_0.

Acknowledgment. We thank the National Science Foundation for supporting the work at Rensselaer under Grant CBT-8608216 and A. G. Slavejkov and W. F. Flaherty for technical assistance. P.M. thanks the Robert A. Welch Foundation (Grant B-1174), the University of North Texas Faculty Research Fund, and B. J. Barron of the UNT Computing Center for their assistance with the theoretical work.

(40) Dunning, T. H., Jr.; Hay, P. J. In *Modern Theoretical Chemistry, Methods of Electronic Structure Theory*; Schaefer, H. F., III, Ed.; Plenum: New York, 1977; Vol. 3, Chapter 1.

(41) Firsch, M. J.; Head-Gordon, M.; Schlegel, H. B.; Raghavachari, K.; Binkley, J. S.; Gonzalez, C.; Defrees, D. J.; Fox, D. J.; Whiteside, R. A.; Seeger, R.; Melius, C. F.; Baker, J.; Martin, R.; Kahn, L. R.; Stewert, J. J. P.; Fluder, E. M.; Topiol, S.; Pople, J. A. *Gaussian 88*; Gaussian: Pittsburgh, PA, 1988.

(42) Hehre, W. J.; Ditchfield, R.; Pople, J. A. *J. Chem. Phys.* **1972**, *56*, 2257.

(43) Besler, B. H.; Sevilla, M. D.; MacNeille, P. *J. Phys. Chem.* **1986**, *90*, 6446.

(44) Boness, M. J. W.; Schulz, G. J. *Phys. Rev. A* **1970**, *2*, 2182.

(45) Celotta, R. J.; Bennet, R. A.; Hall, J. L.; Siegel, M. W.; Levine, J. *Phys. Rev. A* **1972**, *6*, 631.

(46) Allen, W. D.; Horner, D. A.; Dekock, R. L.; Remington, R. B.; Schaefer, H. F., III. *Chem. Phys.* **1989**, *133*, 11.

(47) Andrews, L. *J. Phys. Chem.* **1969**, *73*, 3922.

(48) Adrian, F. J.; Cochran, E. L.; Bowers, V. A. *J. Chem. Phys.* **1973**, *59*, 56.

(49) Use of our ab initio bond lengths would increase the product of the moments of inertia,[14] employed in the equilibrium calculations of section 4.1, by a factor of 1.3. The effect would be to lower the experimental limit to D_0 by less than 2 kJ mol^{-1}.